Supramolecular Chemistry

International Edition: DOI: 10.1002/anie.201605440
German Edition: DOI: 10.1002/ange.201605440

A Halogen-Bond-Induced Triple Helicate Encapsulates Iodide

*Casey J. Massena, Nicholas B. Wageling, Daniel A. Decato, Enrique Martin Rodriguez, Ariana M. Rose, and Orion B. Berryman**

Abstract: *The self-assembly of higher-order anion helicates in solution remains an elusive goal. Herein, we present the first triple helicate to encapsulate iodide in organic and aqueous media as well as the solid state. The triple helicate self-assembles from three tricationic arylethynyl strands and resembles a tubular anion channel lined with nine halogen bond donors. Eight strong iodine···iodide halogen bonds and numerous buried π-surfaces endow the triplex with remarkable stability, even at elevated temperatures. We suggest that the natural rise of a single-strand helix renders its linear halogen-bond donors non-convergent. Thus, the stringent linearity of halogen bonding is a powerful tool for the synthesis of multi-strand anion helicates.*

The helical folding of a molecule confers extraordinary higher-order structure and function. Examples are rife in nature, ranging from the structural role of collagen to the safeguarding of genetic information in polynucleotides. By implementing this privileged pattern, cation-[1] and neutral-guest-[2] induced helices and foldamers[1e,3] have led to myriad applications, including biomolecular and chiral recognition, supramolecular catalysis, and materials. In contrast, the progression of anion helicates, especially those involving multiple strands, has lagged. This delay is understandable given the complexities of guest-induced helical folding, which are magnified by the high solvation energies and variable coordination geometries of anions. To date, a small but growing number of single-strand anion helicates[4] have been synthesized and investigated. However, only four hydrogen-bonding solid-state[5] and three solution-phase[6] duplexes have been developed. Li et al. have produced the only triplex,[7] which enfolded two trianionic phosphates with hydrogen-bonding bis-(biurea) ligands. Only one example of a solid-state halogen-bonding double helicate exists.[8] Herein, we describe an alternative approach to assemble higher-order anion helicates. Exploiting the stringent linearity of halogen bonding, the first triple helicate to bind iodide in solution and the solid state is presented. This cylindrical structure self-assembles from three arylethynyl strands that encircle two iodide anions with halogen bonds. The helix demonstrates remarkable stability at high temperatures and in aqueous and organic solvents. The linearity of halogen bonding facilitates multi-strand complexation and offers a tractable approach to self-assemble large tubular containers with high affinity for complementary anions.

During the last two decades, halogen-bonding molecular hosts[9] have evolved with increasing sophistication, while crystallographic,[10] gas-phase,[11] and biomolecular[11a,b,12] investigations have continued to refine our understanding of this emerging noncovalent bond. A halogen bond is an attractive interaction between an electrophilic region of a halogen atom and a nucleophilic region of an atomic or molecular entity.[10g,13] Although analogous to hydrogen bonding with regard to strength, the halogen bond is far more directional (the angle R–X···Y tends to be close to 180°, where X is a halogen, R a covalently bound group, and Y the halogen-bond acceptor).

Recently, we synthesized a bidentate halogen-bonding receptor (**1**) that demonstrated notable affinity for perrhenate in solution and the solid state (Scheme 1).[14] Receptor

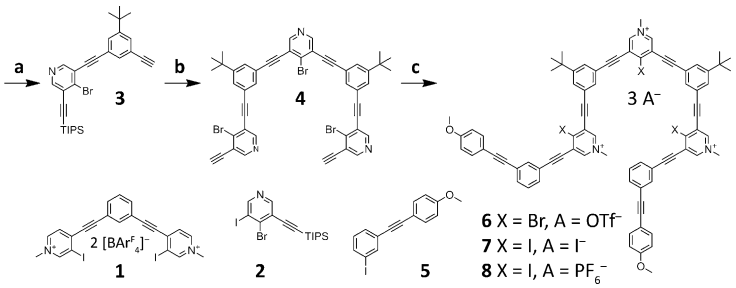

Scheme 1. Synthesis of the bromo- and iodopyridinium nonamers. Reagents and conditions: a) **2**, 1-*tert*-butyl-3,5-diethynylbenzene, $PdCl_2(PPh_3)_2$, CuI, Et_3N, DMF, room temperature, 12 h, 21%; b) 4-bromo-3,5-diiodopyridine, $PdCl_2(PPh_3)_2$, CuI, Et_3N, DMF, 50°C, 12 h, 75%; then TBAF, THF, 0°C to room temperature, 10 min, quantitative; c) **5**, $PdCl_2(PPh_3)_2$, CuI, Et_3N, DMF, 50°C, 24 h, 61%; then MeOTf, CH_2Cl_2, room temperature, 12 h, 93% (**6**); then NaI, 1:3 *v*/*v* DMF-MeCN, room temperature, 12 h, 90% (**7**); then $AgPF_6$, 1:1 *v*/*v* DMF-EtOAc, 30 min, room temperature, 80% (**8**).

1 employed two convergent 3-iodopyridinium halogen-bond donors extending from a 1,3-diethynylbenzene core. Expanding on this design, we envisioned an oligomer with three 4-iodopyridinium halogen-bond donors, spaced by two 1-*tert*-butyl-3,5-diethynylbenzene groups, and capped with two 4-methoxytolan groups. Design principles were drawn from Moore's seminal work with *meta*-phenylene ethynylene foldamers[2e,f,3k,l,15] and Flood's elegant chloride encapsulating double helicate[6a] to encourage the favorable π-stacking of

[*] C. J. Massena, N. B. Wageling, D. A. Decato, E. Martin Rodriguez, A. M. Rose, Prof. Dr. O. B. Berryman
Department of Chemistry and Biochemistry
University of Montana
32 Campus Dr, Missoula, MT 59812 (USA)
E-mail: orion.berryman@umontana.edu

Supporting information and the ORCID identification number(s) for the author(s) of this article can be found under http://dx.doi.org/10.1002/anie.201605440.

alternating electron-deficient and electron-rich aromatic rings. Our departure from previous work is the strategic placement of inwardly directed halogen-bond donors.

Synthesis of the arylethynyl oligomers began with the Sonogashira mono-cross-coupling of known 4-bromo-3,5-diiodopyridine and commercially available (triisopropylsilyl)acetylene to create the monoacetylated halopyridine **2** (Scheme 1). Mono-cross-coupling **2** with known 1-*tert*-butyl-3,5-diethynylbenzene afforded the arylethynyl dimer **3**. Cross-coupling two equivalents of **3** to 4-bromo-3,5-diiodopyridine followed by removing both triisopropylsilyl protecting groups yielded arylethynyl pentamer **4**. Synthesis of the 4-methoxytolan cap **5** was conducted by mono-cross-coupling commercially available 4-ethynylanisole and 1,3-diiodobenzene. Cross-coupling two equivalents of **5** to **4** and subsequent methylation of the bromopyridines with methyl triflate resulted in the tricationic bromopyridinium nonamer **6**. Exchange of the halogens (bromine for iodine) and counteranions (triflate for iodide) was achieved by stirring **6** with excess sodium iodide, providing the iodopyridinium target **7** (for further synthetic details, see Sections S2,S3 in the Supporting Information).

Yellow plates of **7** suitable for X-ray diffraction were grown by the vapor diffusion of methyl-*tert*-butyl ether into a 1:2 *v*/*v* DMF-MeCN solution of **6** and excess tetra-*n*-butylammonium (TBA) iodide.[16] Triple helicate **7** crystallized in space group *C*2/*c*, adopting both *M*- and *P*-helical conformations. Each complex is composed of three intertwined tricationic nonameric strands, offset along a common screw axis as defined by the two intrachannel iodides (Figure 1a). Each iodide is bound tightly by four strong and linear halogen bonds within the helical channel (average halogen-bond I···I$^-$ distance is 3.4 Å, 83% of ΣvdW radii; average C–I···I$^-$ angle is 171°). Consequently, pseudo-square-planar coordination is achieved (Figure 1c). The halogen bonds are complemented by numerous aromatic and ethynyl π-stacking interactions (44 buried aromatic surfaces, Figure 1b; average ring–ring distance is ca. 3.7 Å). Additionally, seven iodides held to the helicate's exterior by ion-pairing interactions help balance the nine positive charges associated with the cationic strands (Figure S23). Each triplex exhibits an approximate height and width of 13 and 19 Å, respectively, and a pitch of 10 Å. Finally, a 2.7 Å pore adorned with halogen-bond donors highlights the unique microenvironment found within the triple helicate (Figures 1a,b). The only molecular axis of symmetry (C_2) for the triplex aligns with the C–I bond of the nonbonding iodopyridinium donor (Figures 1a,c, yellow sticks; for further crystallographic details, see Section S4 in the Supporting Information).

To explore the implications of helical rise and halogen-bond linearity, we calculated the conformation of a single strand of **7** using density functional theory (DFT). The added black dashes and iodides in Figure 1d emphasize the poor preorganization of a single strand. Iodide was placed in this non-convergent binding pocket, and the energies of both tridentate and bidentate halogen bonding were calculated. Regardless of guest placement, nonbonding or repulsive interactions were inevitable (for computational details, see Section S5 in the Supporting Information). These calculations suggest that the strict linearity of halogen bonding disfavors 1:1 binding.

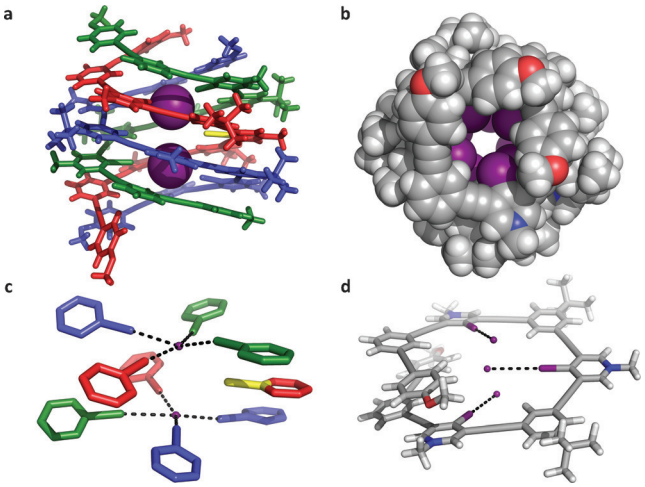

Figure 1. Solid-state representations of triple helicate **7** and DFT-minimized nonamer. a) Solid-state structure of the triple helicate binding two intrachannel iodides. b) Crystal structure of the triplex looking down its anion channel (iodides removed for clarity). c) Pseudo-square-planar coordination geometry of the helicate's halogen-bond donors (scaffolding removed). Black dashes denote halogen bonds. d) DFT-minimized nonamer of **7**. Black dashes and iodides added to emphasize the non-convergence of the halogen-bond donors. In (a)–(c): external iodide atoms removed for clarity. In (a) and (c): yellow C–X stick demarcates the nonbonding halogen-bond donor and axis of molecular C_2 symmetry of the complex. Not all colors are representative of atom identity.

The elucidation of triple helicate **7** in solution began with ^{1}H NMR spectroscopic titrations. Compared to the relatively simple ^{1}H NMR spectrum of **6** in [D$_7$]DMF, the spectrum of triplex **7** suggested a thermodynamically stable aggregate (Figure 2a). Even an excess of TBA bromide failed to convolute the spectrum of **6** (Figure S30). Given the superior halogen-bonding ability of iodines,[9f,10f,11a] these data provided qualitative evidence that **7** persisted as a halogen-bond-induced aggregate. Furthermore, titrating silver hexafluorophosphate ($AgPF_6$)—which precipitated silver iodide leaving non-coordinating PF_6^- anions—to a solution of **7** resulted in complete spectral deconvolution (Figure S31). The isolation of PF_6^- salt **8** (Scheme 1) permitted the reverse titration, holding the concentration of **8** constant while titrating TBA iodide. Surprisingly, even 0.2 equivalents of guest induced significant complex formation that displayed slow exchange with single strands of **7** on the NMR timescale (Figure 2b). The aggregate's pyridinium and anisole signals were markedly shifted upfield (up to −0.79 and −0.54 ppm, respectively; for proton assignments, Figure S32), suggesting significant π-stacking in solution.[2a,3k,l,4a,c,7] With three equivalents of TBA iodide, the resulting ^{1}H NMR spectrum was analogous to that of **7**, indicating strong halogen bonding in solution (Figure 2b).

The 2D NOESY spectrum of triplex **7** provided further evidence of higher-order helication in solution. Strong in-phase cross peaks corresponding to pyridinium methyl and *tert*-butyl signals were consistent with the solid-state structure

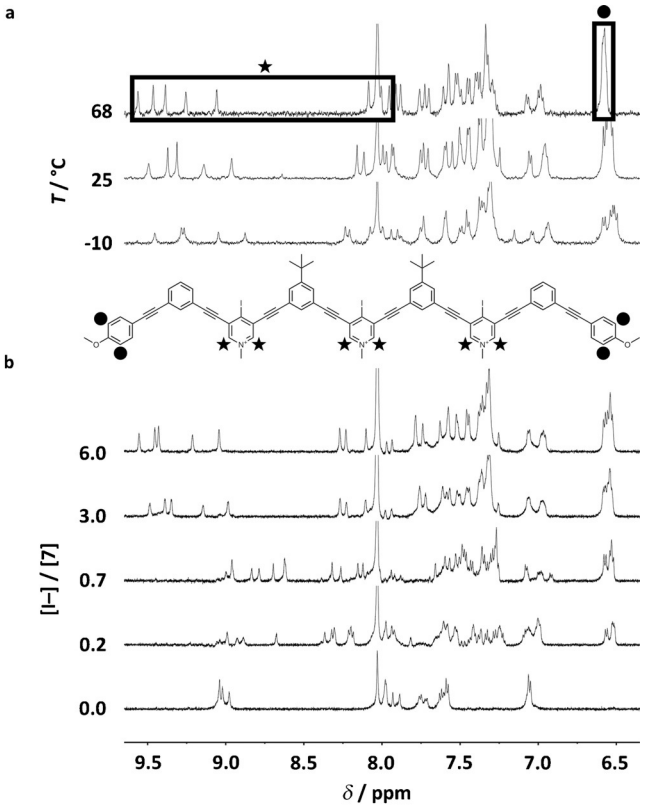

Figure 2. ^{1}H NMR variable temperature and titration experiments. a) ^{1}H NMR spectra of triple helicate **7** subjected to variable temperature (500 MHz, 1:4 *v*/*v* [D_7]DMF–CD_3CN). b) ^{1}H NMR titration involving **8** with additions of TBA iodide (600 MHz, 1:3 *v*/*v* [D_7]DMF–CD_3CN, 298 K).

but impossible for a single strand (over 7 Å apart; Figure S33). Likewise, medium in-phase cross peaks between *tert*-butyl and pyridinium protons as well as *tert*-butylbenzene and pyridinium methyl protons agreed with the X-ray crystal structure but could not originate from a single strand (over 5 and 6 Å apart, respectively). In stark contrast, the 2D NOESY spectrum of **8** manifested none of these features. Instead, only opposite-phase cross peaks between aromatic protons and same-ring substituents were evident, consistent with conformational heterogeneity in solution (Figure S34).

Further comparisons between the ^{1}H NMR spectrum of **7** and its solid-state structure confirmed triple helicate fidelity in solution. The numbers and intensities of ^{1}H NMR signals corresponding to the solid-state triplex were readily predictable due to its molecular C_2 symmetry (Figure S35). The spectrum of **7** should exhibit three *tert*-butyl and three methoxy methyl signals of equal intensities, four equal intensity pyridinium methyl signals and one of half intensity, and nine equal intensity pyridinium signals. The ^{1}H NMR spectrum of **7** is in full agreement with these predictions (Figure S36), indicating solution and solid-state structural congruence. Higher or lower order helicates would produce more or fewer ^{1}H NMR signals, and variations in molecular symmetry would result in altered ratios between peak counts and relative intensities (for further solution and crystallographic structure analysis, see Section S9 in the Supporting Information).

2D DOSY data were collected to further characterize triple helicate **7** in solution. The ^{1}H NMR resonances of **7** and **8** correlated with discrete diffusion coefficient lines, verifying that both species were distinct and monodispersed (Figures S40,S41). Additionally, the hydrodynamic radii (r_H) of **7**, **8**, and an internal standard (dichloromethane) were compared. Unsurprisingly, the r_H of **8** was 1.3-times larger than that of the triple helicate. Given the dynamics of **8** in solution, a r_H inclusive of uncoiled conformations is sensible. In contrast, the π-stacked and coiled conformation of **7** would likely result in a smaller r_H. The triple helicate's estimated r_H of 8 Å agrees with the crystallographic radii of the complex (roughly 6.4 Å height and 9.5 Å width; for details pertaining to DOSY refinement and analysis, see Section S10 in the Supporting Information).

Given that most anion multiplexes require either highly charged anions or low temperatures to form in solution, it was remarkable that the helicate proved stable up to 68 °C (the limit of the probe; Figure 2a). Surmising that halogen bonds are critical for triple helicate stability, we probed them directly with UV/Vis titrations. The UV/Vis spectra of **8** suggested significant conformational changes upon titrating TBA iodide (Figure S42). Gradual depression of the $\lambda =$ 312 nm π–π* band was observed, consistent with the hypochromic effect of π-stacking *meta*-phenylene ethynylene oligomers.[3k,l] Overall, the absorbance decreased by 22 % after titrating two equivalents of guest. Surprisingly, adding as little as 0.01 equivalents of TBA iodide induced half of this total hypochromicity. At higher concentrations of **8**, titrating TBA iodide produced a dark yellow solution associated with the appearance and growth of an absorption band at 400 nm (Figure S43). The absorption band is consistent with halogen-bond charge-transfer in solution.[10f,17] Alongside the demonstrated anion induced folding and denaturing of the triplex, these data implicate halogen bonding as a vital component of helicate formation.

To ascertain triple helicate stability in aqueous phase, **7** was subjected to ^{1}H NMR and 2D NOESY spectroscopy in a 1:1 *v*/*v* D_2O-[D_7]DMF solution (the limit of solubility). Aside from differences in chemical shifts, the spectroscopic features of **7** were fully consistent with those identified in organic solvents (Figures S44,S45). Remarkably, after 20 days in solution **7** exhibited minimal decomposition, notwithstanding the chemical instability of 4-iodopyridiniums (Figure S46). In contrast, residual water hydrolyzed **8** in a matter of hours. The compact and helical conformation of **7** protects the otherwise chemically sensitive 4-iodopyridinium halogen-bond donors. This helix conferred chemical stability is not without precedent.[1c,e]

In conclusion, we have described the first halogen-bond-induced triple helicate to bind iodide in solution and the solid state. The helicate is stabilized by multiple strong and linear halogen bonds and π-stacking interactions. Furthermore, we have demonstrated that the complex is shape-persistent at high temperatures and in aqueous phase. Given the competing speciation and myriad noncovalent interactions in solution, the thorough characterization of a self-assembled triple anion helicate is an important step towards the rational design of large tubular containers with high affinity for complemen-

tary guests. We hypothesize that the combination of helical rise and halogen-bond linearity influences higher-order helication by destabilizing 1:1 complexes. Hence, the expedient self-assembly of a convergent, multidentate halogen-bonding microenvironment may be realized. These results have implications in anion sensing, nanomaterials, and synthetic ion channeling.

Acknowledgements

This work was funded by the Center for Biomolecular Structure and Dynamics CoBRE (NIH NIGMS grant P20GM103546), National Science Foundation (NSF) CAREER CHE-1555324, Montana University System MREDI 51030-MUSRI2015-02, and the University of Montana (UM). The X-ray crystallographic data were collected using a Bruker D8 Venture, principally supported by NSF MRI CHE-1337908. We thank Allen Oliver and Brian Patrick for valuable crystallographic discussions. Funding for shared instrumentation in the CAMCOR NMR Facility at the University of Oregon was provided by NSF Award CHE-0923589 (MRI/ARRA), CHE-1427987 (MRI) with additional support from the Oregon Nanoscience and Microtechnologies Institute (ONAMI), OregonBEST, and the UO Office for Research and Innovation. We thank Klara Briknarova for help with 2D NMR interpretation, Earle Adams for general NMR guidance, Michael Strain for assistance with DOSY NMR collection and refinement, and Valeriy Smirnov and Ian Chrisman for the use of their glovebox.

Keywords: halogen bonding · helical structures · host–guest systems · self-assembly · supramolecular chemistry

How to cite: *Angew. Chem. Int. Ed.* **2016**, *55*, 12398–12402
Angew. Chem. **2016**, *128*, 12586–12590

[1] a) W. Makiguchi, S. Kobayashi, Y. Furusho, E. Yashima, *Angew. Chem. Int. Ed.* **2013**, *52*, 5275; *Angew. Chem.* **2013**, *125*, 5383; b) C. Piguet, M. Borkovec, J. Hamacek, K. Zeckert, *Coord. Chem. Rev.* **2005**, *249*, 705; c) M. J. Hannon, L. J. Childs, *Supramol. Chem.* **2004**, *16*, 7; d) M. Albrecht, *Chem. Rev.* **2001**, *101*, 3457; e) D. J. Hill, M. J. Mio, R. B. Prince, T. S. Hughes, J. S. Moore, *Chem. Rev.* **2001**, *101*, 3893; f) C. Piguet, G. Bernardinelli, G. Hopfgartner, *Chem. Rev.* **1997**, *97*, 2005.

[2] a) H.-G. Jeon, J. Y. Jung, P. Kang, M.-G. Choi, K.-S. Jeong, *J. Am. Chem. Soc.* **2016**, *138*, 92; b) N. Chandramouli, Y. Ferrand, G. Lautrette, B. Kauffmann, C. D. Mackereth, M. Laguerre, D. Dubreuil, I. Huc, *Nat. Chem.* **2015**, *7*, 334; c) Q. Gan, Y. Ferrand, C. Bao, B. Kauffmann, A. Grélard, H. Jiang, I. Huc, *Science* **2011**, *331*, 1172; d) H. Juwarker, J.-m. Suk, K.-S. Jeong, *Chem. Soc. Rev.* **2009**, *38*, 3316; e) A. Tanatani, M. J. Mio, J. S. Moore, *J. Am. Chem. Soc.* **2001**, *123*, 1792; f) R. B. Prince, S. A. Barnes, J. S. Moore, *J. Am. Chem. Soc.* **2000**, *122*, 2758.

[3] a) C. S. Hartley, *Acc. Chem. Res.* **2016**, *49*, 646; b) D.-W. Zhang, X. Zhao, Z.-T. Li, *Acc. Chem. Res.* **2014**, *47*, 1961; c) Y. Zhao, H. Cho, L. Widanapathirana, S. Zhang, *Acc. Chem. Res.* **2013**, *46*, 2763; d) D.-W. Zhang, X. Zhao, J.-L. Hou, Z.-T. Li, *Chem. Rev.* **2012**, *112*, 5271; e) G. Guichard, I. Huc, *Chem. Commun.* **2011**, *47*, 5933; f) A. Roy, P. Prabhakaran, P. K. Baruah, G. J. Sanjayan, *Chem. Commun.* **2011**, *47*, 11593; g) D. Haldar, C. Schmuck, *Chem. Soc. Rev.* **2009**, *38*, 363; h) I. Saraogi, A. D. Hamilton, *Chem. Soc. Rev.* **2009**, *38*, 1726; i) B. Gong, *Acc. Chem. Res.* **2008**, *41*, 1376; j) I. Huc, *Eur. J. Org. Chem.* **2004**, 17; k) R. B. Prince, J. G. Saven, P. G. Wolynes, J. S. Moore, *J. Am. Chem. Soc.* **1999**, *121*, 3114; l) J. C. Nelson, J. G. Saven, J. S. Moore, P. G. Wolynes, *Science* **1997**, *277*, 1793.

[4] a) H. Juwarker, K.-S. Jeong, *Chem. Soc. Rev.* **2010**, *39*, 3664; b) C. A. Johnson, O. B. Berryman, A. C. Sather, L. N. Zakharov, M. M. Haley, D. W. Johnson, *Cryst. Growth Des.* **2009**, *9*, 4247; c) J.-m. Suk, K.-S. Jeong, *J. Am. Chem. Soc.* **2008**, *130*, 11868.

[5] a) P. M. Selvakumar, P. Y. Jebaraj, J. Sahoo, E. Suresh, K. J. Prathap, R. I. Kureshy, P. S. Subramanian, *RSC Adv.* **2012**, *2*, 7689; b) Y. Haketa, H. Maeda, *Chem. Eur. J.* **2011**, *17*, 1485; c) S. J. Coles, J. G. Frey, P. A. Gale, M. B. Hursthouse, M. E. Light, K. Navakhun, G. L. Thomas, *Chem. Commun.* **2003**, 568; d) J. Keegan, P. E. Kruger, M. Nieuwenhuyzen, J. O'Brien, N. Martin, *Chem. Commun.* **2001**, 2192.

[6] a) Y. Hua, Y. Liu, C.-H. Chen, A. H. Flood, *J. Am. Chem. Soc.* **2013**, *135*, 14401; b) H. Maeda, K. Kitaguchi, Y. Haketa, *Chem. Commun.* **2011**, *47*, 9342; c) J. Sánchez-Quesada, C. Seel, P. Prados, J. de Mendoza, I. Dalcol, E. Giralt, *J. Am. Chem. Soc.* **1996**, *118*, 277.

[7] S. Li, C. Jia, B. Wu, Q. Luo, X. Huang, Z. Yang, Q.-S. Li, X.-J. Yang, *Angew. Chem. Int. Ed.* **2011**, *50*, 5721; *Angew. Chem.* **2011**, *123*, 5839.

[8] A. Casnati, R. Liantonio, P. Metrangolo, G. Resnati, R. Ungaro, F. Ugozzoli, *Angew. Chem. Int. Ed.* **2006**, *45*, 1915; *Angew. Chem.* **2006**, *118*, 1949.

[9] a) A. Brown, P. D. Beer, *Chem. Commun.* **2016**, *52*, 8645; b) N. B. Wageling, G. F. Neuhaus, A. M. Rose, D. A. Decato, O. B. Berryman, *Supramol. Chem.* **2016**, *28*, 665; c) N. K. Beyeh, F. Pan, K. Rissanen, *Angew. Chem. Int. Ed.* **2015**, *54*, 7303; *Angew. Chem.* **2015**, *127*, 7411; d) O. Dumele, N. Trapp, F. Diederich, *Angew. Chem. Int. Ed.* **2015**, *54*, 12339; *Angew. Chem.* **2015**, *127*, 12516; e) L. C. Gilday, S. W. Robinson, T. A. Barendt, M. J. Langton, B. R. Mullaney, P. D. Beer, *Chem. Rev.* **2015**, *115*, 7118; f) A. V. Jentzsch, *Pure Appl. Chem.* **2015**, *87*, 15; g) T. M. Beale, M. G. Chudzinski, M. G. Sarwar, M. S. Taylor, *Chem. Soc. Rev.* **2013**, *42*, 1667; h) M. Erdélyi, *Chem. Soc. Rev.* **2012**, *41*, 3547; i) S. M. Walter, F. Kniep, E. Herdtweck, S. M. Huber, *Angew. Chem. Int. Ed.* **2011**, *50*, 7187; *Angew. Chem.* **2011**, *123*, 7325; j) M. G. Sarwar, B. Dragisic, S. Sagoo, M. S. Taylor, *Angew. Chem. Int. Ed.* **2010**, *49*, 1674; *Angew. Chem.* **2010**, *122*, 1718.

[10] a) A. Mukherjee, S. Tothadi, G. R. Desiraju, *Acc. Chem. Res.* **2014**, *47*, 2514; b) R. W. Troff, T. Mäkelä, F. Topić, A. Valkonen, K. Raatikainen, K. Rissanen, *Eur. J. Org. Chem.* **2013**, 1617; c) G. Cavallo, P. Metrangolo, T. Pilati, G. Resnati, M. Sansotera, G. Terraneo, *Chem. Soc. Rev.* **2010**, *39*, 3772; d) C. B. Aakeröy, N. C. Schultheiss, A. Rajbanshi, J. Desper, C. Moore, *Cryst. Growth Des.* **2009**, *9*, 432; e) M. Fourmigué, *Curr. Opin. Solid State Mater. Sci.* **2009**, *13*, 36; f) P. Metrangolo, F. Meyer, T. Pilati, G. Resnati, G. Terraneo, *Angew. Chem. Int. Ed.* **2008**, *47*, 6114; *Angew. Chem.* **2008**, *120*, 6206; g) P. Metrangolo, H. Neukirch, T. Pilati, G. Resnati, *Acc. Chem. Res.* **2005**, *38*, 386; h) R. B. Walsh, C. W. Padgett, P. Metrangolo, G. Resnati, T. W. Hanks, W. T. Pennington, *Cryst. Growth Des.* **2001**, *1*, 165.

[11] a) M. R. Scholfield, C. M. V. Zanden, M. Carter, P. S. Ho, *Protein Sci.* **2013**, *22*, 139; b) R. Wilcken, M. O. Zimmermann, A. Lange, A. C. Joerger, F. M. Boeckler, *J. Med. Chem.* **2013**, *56*, 1363; c) P. Politzer, J. S. Murray, T. Clark, *Phys. Chem. Chem. Phys.* **2010**, *12*, 7748; d) K. E. Riley, J. S. Murray, P. Politzer, M. C. Concha, P. Hobza, *J. Chem. Theory Comput.* **2009**, *5*, 155; e) A. C. Legon in *Halogen Bonding: Fundamentals and Applications* (Eds.: P. Metrangolo, G. Resnati), Springer, Berlin, **2008**, p. 17; f) J. W. Zou, Y. J. Jiang, M. Guo, G. X. Hu, B. Zhang, H. C. Liu, Q. S. Yu, *Chem. Eur. J.* **2005**, *11*, 740.

[12] Y. Lu, T. Shi, Y. Wang, H. Yang, X. Yan, X. Luo, H. Jiang, W. Zhu, *J. Med. Chem.* **2009**, *52*, 2854.
[13] G. R. Desiraju, P. S. Ho, L. Kloo, A. C. Legon, R. Marquardt, P. Metrangolo, P. Politzer, G. Resnati, K. Rissanen, *Pure Appl. Chem.* **2013**, *85*, 1711.
[14] C. J. Massena, A. M. S. Riel, G. F. Neuhaus, D. A. Decato, O. B. Berryman, *Chem. Commun.* **2015**, *51*, 1417.
[15] K. Matsuda, M. T. Stone, J. S. Moore, *J. Am. Chem. Soc.* **2002**, *124*, 11836.
[16] Crystallographic Data for **7** $C_{80}H_{61}I_6N_3O_2$, $M_r = 1857.71$, monoclinic, space group *C2/c* (no. 15), $a = 54.1200(19)$, $b = 36.8537(14)$, $c = 35.419(2)$, $\beta = 128.1810(10)$, $V = 55530(5)$, $Z = 24$, $T = 100$ K, $\mu(Cu_{K\alpha}) = 16.102\ mm^{-1}$, $D_{calcd} = 1.333\ g\,mL^{-1}$, $2\theta max = 101.124$, 291827 reflections collected, 29038 unique ($R_{int} = 0.0668$, $R_{sigma} = 0.0322$), $R1 = 0.0837$ ($I > 2\sigma(I)$), $wR2 = 0.2858$ (all data). See Section S4 in the Supporting Information. CCDC 1476727 contains the supplementary crystallographic data for this paper. These data can be obtained free of charge from The Cambridge Crystallographic Data Centre via www.ccdc.cam.ac.uk/data_request/cif.
[17] S. V. Rosokha, I. S. Neretin, T. Y. Rosokha, J. Hecht, J. K. Kochi, *Heteroat. Chem.* **2006**, *17*, 449.

Received: June 3, 2016
Published online: July 13, 2016

